Journal of Catalysis **181,** 189–204 (1999)
Article ID jcat.1998.2303, available online at http://www.idealibrary.com on IDEAL®

NO Reduction by CH_4 in the Presence of O_2 over Pd-H-ZSM-5

Lisa J. Lobree, Adam W. Aylor, Jeffrey A. Reimer, and Alexis T. Bell[1]

Chemical Sciences Division, Lawrence Berkeley National Laboratory, and Department of Chemical Engineering, University of California, Berkeley, California 94720

Received March 31, 1998; revised October 5, 1998; accepted October 14, 1998

An investigation of the interaction of NO and NO_2 with Pd-H-ZSM-5, as well as the reduction of NO by CH_4, has been conducted using mass spectrometry and *in situ* infrared spectroscopy. Prior to reaction most of the Pd in Pd-H-ZSM-5 (Pd/Al = 0.048) is present as Pd^{2+} cations. NO reduction by CH_4 in the absence of O_2 results in the progressive reduction of Pd^{2+} cations above 610 K and the formation of small Pd particles. Reduction of Pd^{2+} cations is significantly suppressed when O_2 is added to the feed of NO and CH_4. *In situ* infrared spectroscopy reveals the presence of NO^+ and NO as the principal adsorbed species. NO^+ is present as a charge-compensating cation (e.g., Z^-NO^+) and is believed to be formed via the reaction $2\ Z^-H^+ + 2\ NO + 1/2\ O_2 = 2\ Z^-NO^+ + H_2O$. NO^+ does not react with CH_4 at temperatures up to 773 K. Adsorbed NO reacts with CH_4 above 650 K and CN species are observed as intermediates. The latter species react with both NO, O_2, and presumably NO_2. Based on the accumulated data, a mechanism is proposed to explain the reduction of NO by CH_4 both in the presence and absence of O_2. © 1999 Academic Press

INTRODUCTION

Since Pd-H-ZSM-5 was first reported to be effective for NO reduction by CH_4 in the presence of O_2 (1), there has been considerable interest in understanding the state of Pd in this catalyst. Work by several authors (1–4) has shown that Brønsted acidity is necessary for NO reduction to occur on Pd-exchanged ZSM-5 when O_2 is present. It has also been determined that the activity of Pd-H-ZSM-5 exhibits a maximum with Pd loading at about 0.5 wt% (3, 5), and that Pd exchanged into Na-ZSM-5 shows no activity for NO reduction in the presence of O_2, but remains active for CH_4 combustion (1, 2, 4). XANES and EXAFS studies (6) have shown that at low loadings (0.3 wt%), Pd-H-ZSM-5 exposed to a reaction mixture containing NO, CH_4, and O_2 contains isolated Pd cations each of which is associated with a single O atom. By contrast, a high loaded sample (1.0 wt%) contains primarily clusters of PdO. Similar conclusions have been drawn from infrared investigations of CO and NO adsorption on reduced and oxidized Pd-H-ZSM-5 (7). Based on these studies, it was inferred that highly dispersed Pd is stabilized as $Z^-H^+[PdO]H^+Z^-$ (where Z^- represents a cation exchange site) in portions of the zeolite where there are two Al atoms located in next-nearest neighbor T sites. More recently, density functional theory calculations have shown that the dispersed cations are better represented by the structure $Z^-H^+[Pd(OH)]^+Z^-$ in which one of the two protons is present as an OH group bonded to Pd^{2+} (8). The authors of Ref. (4) have also concluded that protons are required to stabilize Pd^{2+} cations in ZSM-5.

Mechanistic inferences about the reduction of NO by CH_4 in the presence of O_2 over Pd-H-ZSM-5 have been based for the most part on activity measurements. NO_2 has been proposed (2, 9, 10) as a key intermediate since a mixture of NO_2 and CH_4 reacts more rapidly than a mixture containing NO, O_2, and CH_4. The mechanism of NO reduction is envisioned as (1) NO is oxidized in O_2 to NO_2 by either Pd or H^+ while CH_4 is activated independently to form CH_x by reaction with Pd; (2) NO_2 and CH_x react at H^+ sites to form N_2 and CO_x; and (3) CH_x and O_2 react non-selectively at Pd sites to form CO_x. Isotopic labeling experiments suggest that there is no definitive rate-limiting step in the proposed mechanism. While plausible, this mechanism is inconsistent with the observation that there is a slight increase in the rate of NO conversion to N_2 when the concentration of O_2 in the feed is varied from 0.2 to 2%; however, above 2% O_2, the conversion decreases significantly (3, 5). Since the reaction of NO with O_2 to produce NO_2 should proceed with increasing concentration of O_2, these latter observations raise some question about the role of NO_2 as an intermediate in the reduction of NO over Pd-H-ZSM-5. More recently, it has been proposed that while the protons in Pd-H-ZSM-5 are not involved in H abstraction from CH_4, they may participate in subsequent steps, suggesting that both Pd^{2+} and H^+ are required for the selective catalytic reduction of NO by CH_4 (4).

The goal of the present work was to determine surface species present under reaction conditions, and to investigate the interactions of adsorbed NO and NO_2 with CH_4. *In situ* infrared spectroscopy, together with temperature-programmed desorption (TPD) and reaction (TPR)

---

[1] Corresponding author. E-mail: bell@cchem.berkeley.edu.

0021-9517/99 $30.00
Copyright © 1999 by Academic Press
All rights of reproduction in any form reserved.

spectroscopy, was used to elucidate the nature of adsorbed species present on Pd-H-ZSM-5 and to investigate the mechanism of NO reduction by CH_4 in the presence and absence of O_2.

EXPERIMENTAL

Na-ZSM-5 obtained from UOP was converted to the NH_4^+ form. About 15 g of the zeolite was added to a 180 mL solution of 1.0 *M* ammonium nitrate solution. This mixture was stirred at 298 K for 24 h, then filtered, and washed. The procedure was repeated two more times. The resultant NH_4^+-ZSM-5 was added to a 125 mL solution of 0.005 *M* $Pd(NO_3)2 \times H_2O$ at 333 K. This solution was stirred for 36 h (5) then filtered, washed, and dried overnight in a vacuum oven at 393 K. Based on elemental analysis, the Si/Al ratio was determined to be 16.1, and the Pd/Al ratio was determined to be 0.048 (0.44 wt%). Finally, a portion of the unexchanged NH_4^+-ZSM-5 was heated at 773 K in He to convert it to H-ZSM-5.

For infrared spectroscopy, 20–50 mg of the palladium-exchanged zeolite was pressed into a self-supporting wafer and placed into an infrared cell similar to that described by Joly *et al.* (11). Spectra were recorded on a Digilab FTS-50 Fourier-transform infrared spectrometer at a resolution of 4 cm^{-1}. Typically, 64 or 256 scans were coadded to obtain a good signal-to-noise ratio. A reference spectrum of Pd-H-ZSM-5 in He, taken at the same temperature as the experimental spectrum, was subtracted from each spectrum. The temperature was increased at 1.0 K/min during the temperature programmed-infrared spectroscopy (TPD-IR) experiments.

Separate temperature-programmed desorption and reaction (TPD-MS and TPR-MS) experiments were carried out with 0.1 g catalyst sieved to 35–60 mesh and placed in a quartz microreactor. For these experiments, 5000 ppm NO (^{15}NO was used instead of ^{14}NO to minimize the overlap of cracked species) in He was adsorbed on the catalyst at room temperature. The catalyst was purged with He for 1 h to remove weakly adsorbed NO, and then a temperature ramp of 8.0 K/min was initiated. NO was desorbed into either He, 1% O_2 in He, 1% CH_4 in He, or 1% $CH_4 + 1\%$ O_2 in He flowing at 100 cm^3/min; desorbing species were monitored via mass spectrometry (UTI 100 C). Cracking patterns were obtained for all relevant species and the collected data were corrected using this information.

For the present studies, 4.99% NO in He, 1.03% NO_2 in He, 10.1% O_2 in He, and 1.01% CH_4 in He were obtained from Matheson. ^{15}NO and $^{13}CH_4$ were obtained from Isotec. UHP Helium was obtained on-site. The He, NO, and CH_4 gases were passed through an oxysorb trap, and ascarite trap, and a molecular sieve trap, in that order, for additional purification. The O_2 was passed through an ascarite and a molecular sieve trap.

The freshly Pd-exchanged sample was heated at 773 K in He for 8 h to convert all residual NH_4^+ cations to H^+. Prior to each experiment the catalyst was (1) heated at 773 K for 1 h in a He stream containing 5000 ppm NO, (2) heated at 773 K for 2 h in 10% O_2, (3) heated at 773 K in He for 1 h, and (4) cooled to the desired temperature in helium. In the text, this pretreatment will be referred to as a standard pretreatment (S). This complicated pretreatment is based on our previous work (7) which showed that Pd is quite mobile in H-ZSM-5 and that repetitive He pretreatments followed by temperature-programmed desorption experiments resulted in a decrease in Pd dispersion. However, high temperature treatment in NO resulted in a complete redispersion of the Pd.

The catalyst was placed in a quartz microreactor to determine its activity. Reactants were supplied via mass flow controllers and the product composition was determined by gas chromatography. A molecular sieve 5A column was used to separate NO, O_2, N_2, CO, and CH_4. A Porapak Q column was also employed to separate CO_2 and N_2O. Typical reaction mixtures contained 5000 ppm NO, 5000 ppm CH_4, and 2.0% O_2, with the balance He. A 0.20-g sample of the catalyst was used with a total flow rate of 100 cm^3/min, resulting in a $GHSV = 15{,}000$ (based on an apparent bulk density of the zeolite of 0.5 g/cm^3). The conversion of NO was based on the amount of N_2 formed and the conversion of CH_4 was based on the amount of CO_2 and CO formed.

RESULTS

Activity Measurements

Plots of NO and CH_4 conversion versus temperature obtained with and without O_2 present are shown in Fig. 1. At temperatures greater than 723 K, the activity for NO reduction is higher in the absence of O_2, in contrast to what has been observed previously on Co- and Mn-exchanged ZSM-5 (12, 13), but in agreement with recent observations for 0.75 wt% Pd-H-ZSM-5 (3). Reaction begins to occur at approximately 673 K in the absence of O_2, while reaction in O_2 occurs beginning at 623 K. The absence of O_2 leads to the incomplete oxidation of CH_4 as evidenced by the presence of CO. Figure 2 shows the activity of H-ZSM-5 for NO reduction by CH_4 in the presence of O_2. The activity of H-ZSM-5 at 673 K is comparable to the activity of Pd-H-ZSM-5 in the absence of O_2 at the same temperature. However, as the temperature is increased, no significant increase in NO conversion is observed for H-ZSM-5. At 823 K the consumption of NO to form N_2 is approximately three times larger for Pd-H-ZSM-5. At this temperature, the turnover frequencies for Pd-H-ZSM-5 and H-ZSM-5 (based on the assumption of $Pd/Al = 0.048$ and $H/Al = 1.0$) are 5.0×10^{-3} and 1.4×10^{-4} s^{-1}, respectively.

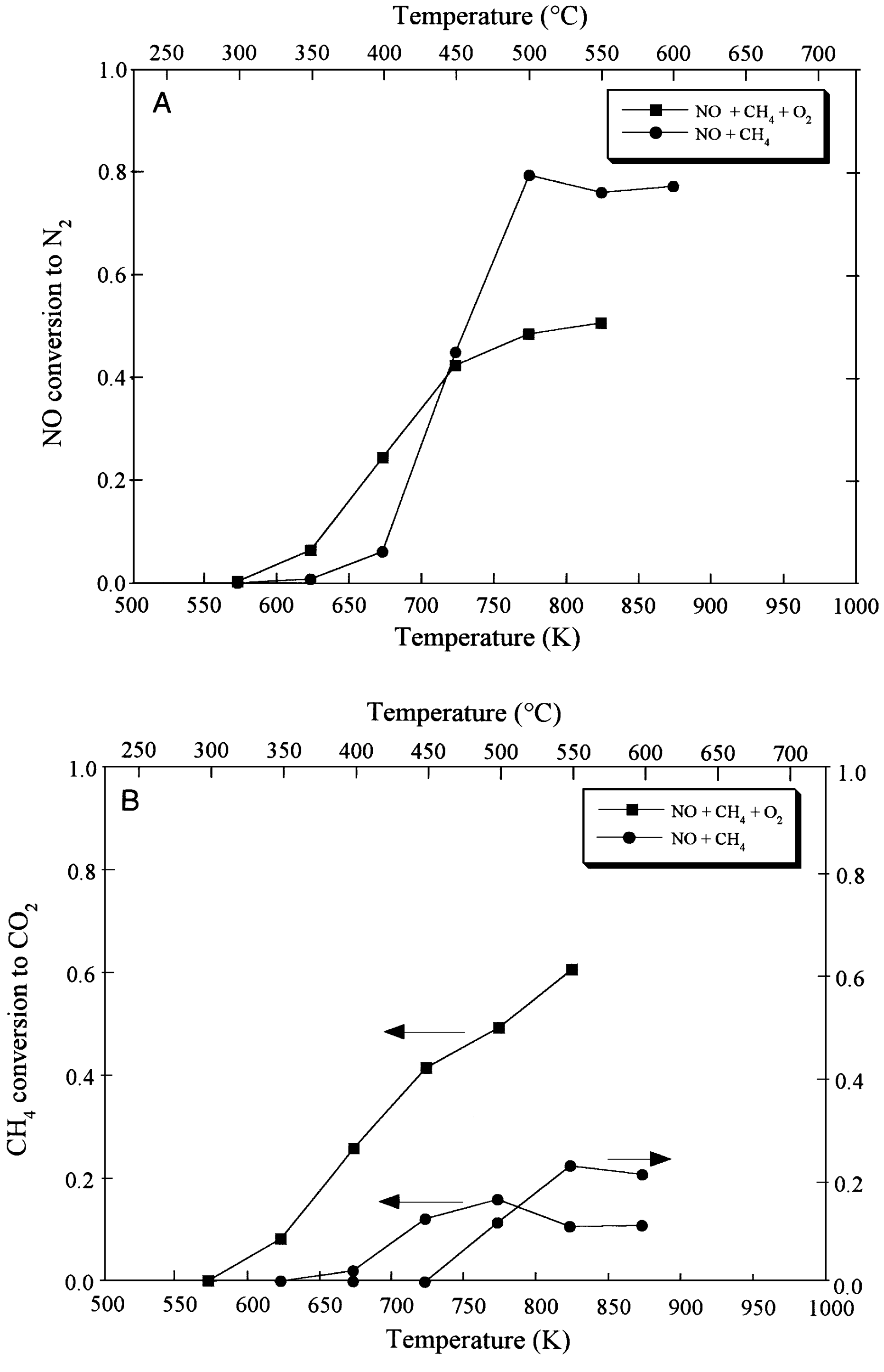

FIG. 1. (A) NO conversion to N_2 on Pd-H-ZSM-5 as a function of temperature. [NO] = 5000 ppm, [CH_4] = 5000 ppm, [O_2] = 2.0%. Total flow rate = 100 cm^3/min, GHSV = 15,000. (B) CH_4 conversion on Pd-H-ZSM-5 as a function of temperature. [NO] = 5000 ppm, [CH_4] = 5000 ppm, [O_2] = 2.0%. Total flow rate = 100 cm^3/min, GHSV = 15,000.

The state of Pd in the catalyst (e.g., as fully dispersed Pd^{2+} cations or as small Pd clusters) can be determined by temperature-programmed desorption of CO (7). Pd fully dispersed as Z^-H^+ $[Pd(OH)]^+Z^-$ can adsorb 1.0 mol CO/mol Pd. However, upon reduction the Pd forms small metal crystallites within the zeolite and the CO adsorption capacity decreases to 0.05 mol CO/mol Pd. This information can be used to ascertain the state of Pd in Pd-H-ZSM-5 at various temperatures following exposure of the catalyst to gas mixtures of NO/CH_4 and $NO/CH_4/O_2$.

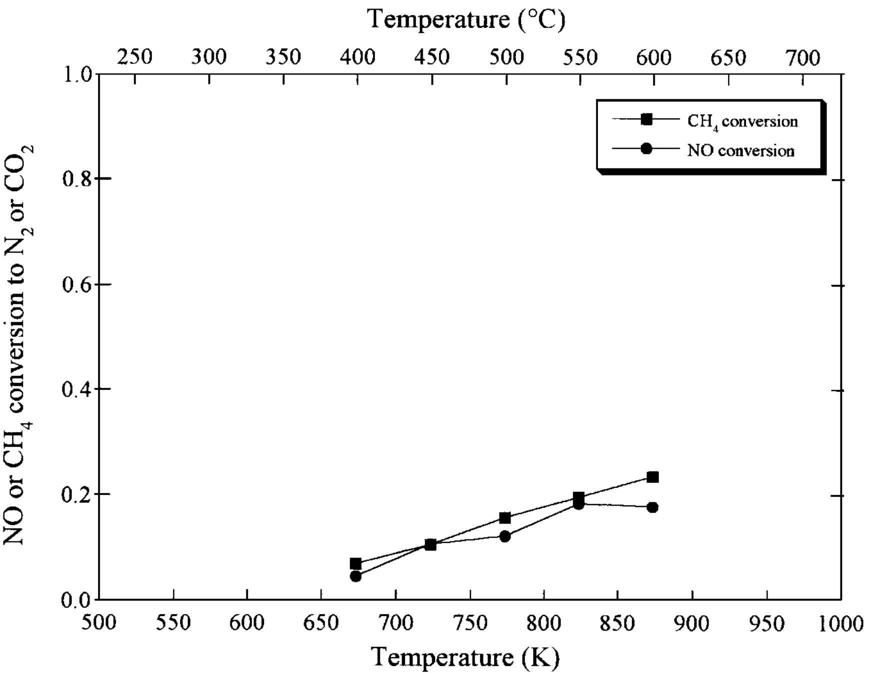

FIG. 2. NO conversion to N_2 and CH_4 conversion to CO_2 on H-ZSM-5 as a function of temperature. [NO] = 5000 ppm, [CH_4] = 5000 ppm, [O_2] = 2.0%. Total flow rate = 100 cm^3/min, GHSV = 15,000.

Figure 3 shows the results of CO TPD experiments used to ascertain the state of the catalyst following exposure to different conditions. The data are plotted as moles of CO adsorbed per mole of Pd as a function of catalyst treatment. Following a standard pretreatment, designated as S1, the sample adsorbs 0.65 mol CO/mol Pd. Since the maximum ratio of CO/Pd is ~1.0 for Pd fully dispersed as Pd^{2+} cations, the observed CO/Pd ratio suggests that only 65% of the Pd is

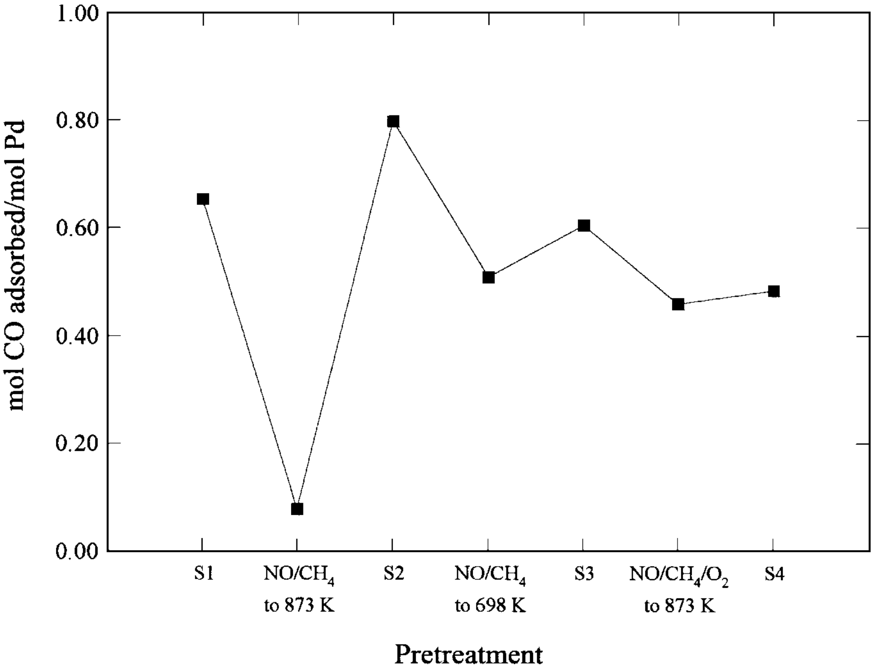

FIG. 3. Amount of CO adsorbed/Pd determined from temperature-programmed desorption in He following room-temperature exposure of Pd-H-ZSM-5 to 4000 ppm CO after various treatments.

present as Pd^{2+} cations following a standard pretreatment. This is not unexpected in as much as prior to the measurements reported in Fig. 3, the catalyst had undergone usage under both oxidizing and reducing conditions.

Following pretreatment S1, the catalyst was exposed to a gas mixture containing 5000 ppm of NO and 5000 ppm of CH_4. The temperature was raised at 2 K/min from 573 to 873 K and then held at 873 K for 1 h. All adsorbed species were desorbed from the catalyst by purging in He for 1 h at 873 K. CO adsorption and TPD were performed after first cooling the catalyst to room temperature. Figure 3 shows that in this case $CO/Pd = 0.08$, suggesting that most of the cation-exchanged Pd has been reduced. A repeat of the standard pretreatment (S2) results in a redispersion of the agglomerated Pd, since the CO/Pd ratio now rises to 0.80. If reaction in NO/CH_4 is allowed to occur again but at a maximum temperature of 698 K, then the CO/Pd ratio determined from CO TPD is now 0.50. This indicates that at 698 K much less of the cation-exchanged Pd has undergone reduction than at 873 K. Repetition of the standard pretreatment a third time (S3) raises the CO/Pd ratio to 0.60. Subsequent reaction of a feed containing 5000 ppm NO, 5000 ppm CH_4, and 2% O_2, followed by CO TPD shows that the CO/Pd ratio now decreases to 0.45. Finally, repetition of the standard pretreatment a fourth time (S4) raises the CO/Pd ratio to 0.50.

It is evident from the results presented in Fig. 3 that cation-exchanged Pd in Pd-H-ZSM-5 can undergo reduction during NO reduction by CH_4. The extent of NO reduction is a function of both the reaction temperature and the presence or absence of O_2 in the feed. High reaction temperatures and the absence of O_2 are conducive to reduction of the cation-exchanged Pd. While the standard pretreatment can redisperse the agglomerated Pd, with repeated use of the catalyst it becomes more difficult to do so. This is very likely a consequence of the formation of progressively larger Pd particles, some of which may be present on the external surface of the ZSM-5 crystallites.

NO TPD in He and O_2

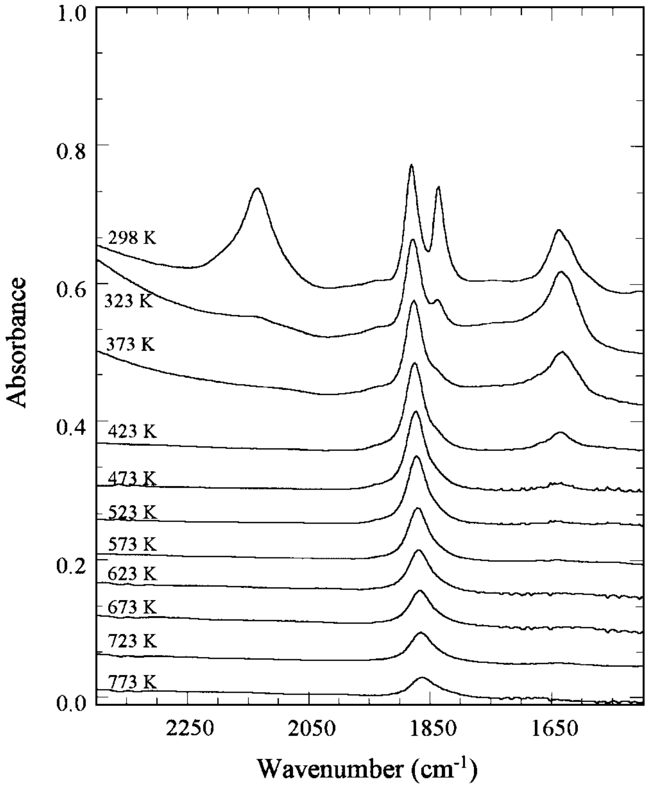

FIG. 4. Infrared spectra taken during temperature-programmed desorption into He following room-temperature exposure of the catalyst to 5000 ppm NO for 20 min.

Figure 4 shows a series of infrared spectra taken during temperature-programmed heating of the catalyst in He after it has been exposed to 5000 ppm NO for 20 min at room temperature. Such experiments are designated TPD-IR experiments. NO adsorption at room temperature results in four bands at 2133, 1881, 1836, and 1638 cm^{-1}. While the bands at 1881 and 1836 cm^{-1} do not change with time, the intensity of the bands at 2133 cm^{-1} and 1638 cm^{-1} both increase with time. The band at 1881 cm^{-1} has been previously assigned to NO adsorbed on Pd cations adjacent to two framework Al atoms (e.g., $Z^-H^+[Pd(OH)(NO)]^+Z^-$) (7). It has been suggested that the band at 1836 cm^{-1} is also due to a nitrosyl group, but that in this case there is another species present at the same site (either NO_2 or H_2O) (14). The concurrent appearance of the bands at 2133 cm^{-1} and 1638 cm^{-1} has been observed previously (13). While the feature at 1638 cm^{-1} is best assigned to H_2O interacting with Brønsted acid sites (15), the assignment of the feature at 2133 cm^{-1} has been the subject of some discussion in the recent literature (16–19). Most investigators have attributed this band to NO_2^+ (19) or $NO_2^{\delta+}$ (16, 17); however, strong evidence has been presented recently (20) for the assignment of this band to NO^+ acting as the charge compensating species at a cation exchange site [e.g., Z^-NO^+] in which the formation of Z^-NO^+ is proposed to occur via the following equilibrium:

$$2\,NO + 1/2\,O_2 + 2\,Z^-H^+ \rightleftharpoons H_2O + 2\,Z\text{-}NO^+.$$

Elevating the temperature causes the disappearance of the band at 2133 cm^{-1} by 373 K. The features at 1836 cm^{-1} and 1638 cm^{-1} are gone above 473 K, while the band at 1881 cm^{-1} persists to 773 K. Note that the feature at 1881 cm^{-1} slowly shifts in frequency as the temperature increases and is located at 1860 cm^{-1} by 773 K. Replacing the He carrier gas with 1% O_2 yields results which are similar to those observed in Fig. 4 up to 673 K. Above this temperature, however, the intensity of the band at 1881 cm^{-1} due to NO adsorbed on Pd is smaller in the presence of O_2.

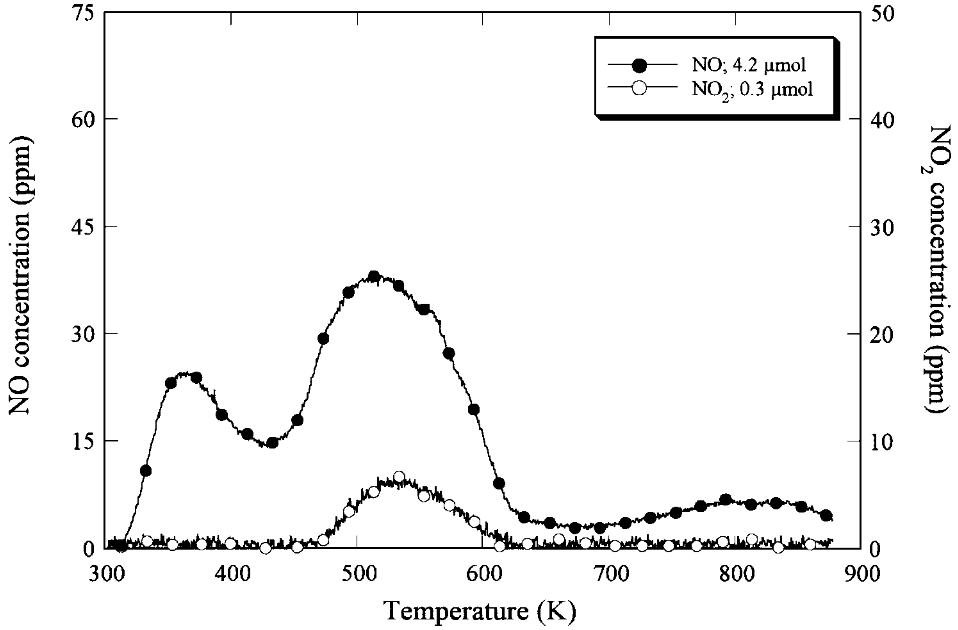

FIG. 5. Mass spectrometer signals for NO and NO_2 observed during temperature-programmed desorption into He following room-temperature exposure of the catalyst to 5000 ppm NO for 20 min. The total quantities of NO and NO_2 desorbed are given in the inset.

The temperature-programmed desorption of NO (TPD-MS) is shown in Fig. 5. Prior to this experiment the catalyst is exposed to 5000 ppm NO in He for 20 min at room temperature, after which the catalyst is purged in He prior to the onset of the temperature ramp. The total amounts of NO and NO_2 desorbing are given in the figure legend. NO desorbs over the entire temperature range, with peaks evident at 365 K, 515 K, and a tail which begins at 675 K and continues to temperatures greater than 873 K. NO_2 desorbs in one peak at 535 K. The total amount of nitrogen (as N) observed to desorb up to 873 K is 4.5 μmol or 1.09 mol N/mol Pd.

While not shown, the TPD spectrum of NO (TPD-MS) recorded in the presence of O_2 is similar to that observed in He with a few exceptions. The quantity of NO_2 desorbing in the presence of O_2 is three times that observed in He, suggesting a transformation of some of the adsorbed NO to NO_2. However, there is no increase in species due to adsorbed NO_2 observed in the infrared spectra, leading to the deduction that NO_2 is formed during NO desorption. Also, consistent with the infrared results, it is observed that in the presence of O_2, all of the NO is desorbed by 873 K. The total amount of nitrogen desorbing is 5.2 μmol, which is equivalent to 1.26 mol N/mol Pd. Since nitrogen-containing species are not observed above 873 K in the TPD-MS or TPD-IR experiments, this quantity is representative of the total amount of NO adsorbed in any NO TPD experiment.

NO TPD in CH_4 and $CH_4 + O_2$

Figure 6A shows a series of spectra taken during the temperature-programmed desorption of NO (TPD-IR) into a stream containing 1% CH_4 in He following the room-temperature adsorption of NO from a stream containing 5000 ppm NO in He. Below 473 K, the spectra look quite similar to those shown in Fig. 4. At higher temperatures, the band at 1881 cm^{-1} (due to $Z^-H^+[Pd(OH)(NO)]^+Z^-$) is first higher in CH_4, then drops to zero above 673 K. Figure 6B shows a blowup of the spectral region between 2000 and 2400 cm^{-1} for temperatures between 673 K and 773 K. At 723 K, new bands can be discerned at 2300 and 2142 cm^{-1}.

In order to identify the adsorbed species yielding the bands at 2300 and 2142 cm^{-1}, isothermal, transient-response experiments were performed at 723 K by preadsorbing ^{15}NO or ^{14}NO and then exposing the sample to $^{12}CH_4$ (^{15}NO) or $^{13}CH_4$ (^{14}NO). The reaction of adsorbed ^{15}NO with $^{12}CH_4$ shifted the position of the bands previously observed at 2300 and 2142 cm^{-1} to 2274 and 2108 cm^{-1}, respectively. By contrast, the reaction of adsorbed ^{14}NO with $^{13}CH_4$ shifted these bands to 2251 and 2100 cm^{-1}. The redshift observed for both bands when one of the gases is isotopically labeled indicates that both species contain N and C atoms. The predicted shifts, treating both adsorbed CN and NCO as pseudo-diatomics, are in close agreement with the assignment of the band at 2142 cm^{-1} to Pd^{2+}-CN. The predicted shifts for the band appearing at 2300 cm^{-1} are consistent with either CN or NCO. The position of the band, however, favors its assignment to NCO. The assignment of the bands at 2300 and 2142 cm^{-1} to adsorbed NCO and CN species, respectively, is consistent with bands previously observed on Co- and Mn-ZSM-5 (13, 21).

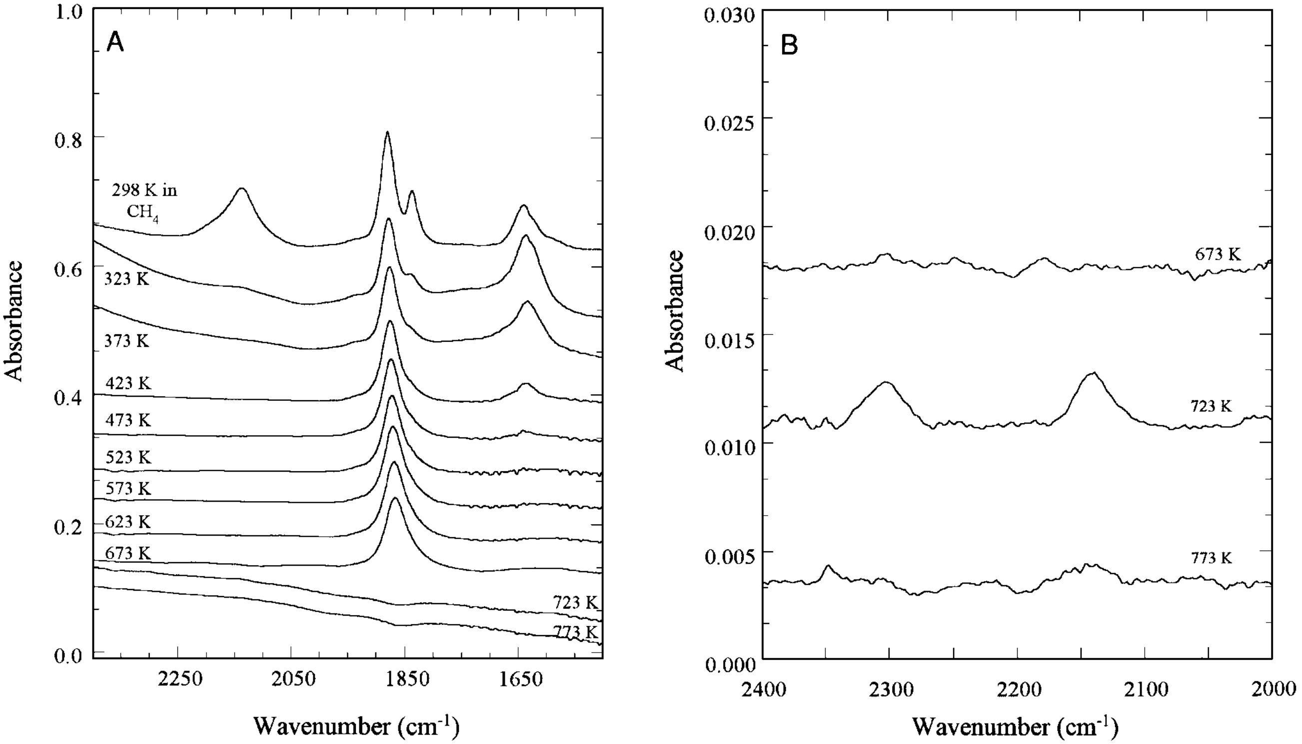

FIG. 6. (A) Infrared spectra taken during temperature-programmed desorption into 1% CH_4 in He following room-temperature exposure of the catalyst to 5000 ppm NO for 20 min. (B) Blowup of spectra taken at 673 K and above during temperature-programmed desorption into 1% CH_4 in He following room-temperature exposure of the catalyst to 5000 ppm NO for 20 min.

While not shown, the temperature-programmed desorption of NO (TPD-IR) into a stream containing 1% CH_4 + 1% O_2 is similar to the TPD into 1% CH_4 up to 673 K. However, the intensity of the nitrosyl band at 1881 cm^{-1} does not decrease very rapidly with increasing temperature above 673 K and the only species observed on the surface between 2000 and 2400 cm^{-1} is due to CO_2 at 2347 cm^{-1}.

Figure 7 shows the spectra acquired during the temperature-programmed desorption of NO (TPD-MS) into a stream containing 1% CH_4 in He taken after exposing the catalyst to 5000 ppm NO at room temperature for 20 min. NO and NO_2 desorption profiles are shown in Fig. 7A. Below 500 K, the desorption spectrum of NO is similar to that seen in Fig. 5. Above this temperature, significantly less NO desorbs, and the nitrosyl species that previously desorbed up to 873 K, are now gone by 740 K. Note also that, in contrast to what is observed in Fig. 5, no NO_2 is seen in the product gases. Figure 7B shows the TPD spectra for CO_2, N_2, and CO production, and for CH_4 consumption. CO is formed over the entire temperature range of the experiment. CO_2 and N_2 are observed in approximately equal concentrations between 460 and 600 K and reach a maximum concentration in this range at 560 K. The absence of NO_2 in the products over this temperature range and the appearance of CO_2 in an amount equivalent to the amount of NO_2 seen to desorb in Fig. 5 suggests that CH_4 reduces NO_2 via the reaction $2NO_2 + CH_4 \rightarrow N_2 + CO_2 + 2H_2O$. The amount of N_2 formed is somewhat less than expected, and the reason for this discrepancy is not clear. CO_2 and N_2 are observed again above 650 K. The CO_2 and N_2 concentrations reach maxima at 700 K, while the CO lags slightly behind and is observed to have a maximum rate at 710 K. The amounts of N_2 and CO_2 produced in the temperature interval of 650–720 K are noted in Fig. 7B. Also listed is the amount of CO produced above and beyond the amount produced by the reduction of the catalyst (see below). The ratio of N_2 to CO_x produced over the temperature interval of 650–720 K is 1.2. Finally, it is noted that the total amount of nitrogen products desorbing from the catalyst (measured as moles of N) is 5.1 μmol, in good agreement with the maximum amount of N adsorbed.

To assess whether the large amount of CO observed in Fig. 7B above 675 K was due to the reduction of the catalyst by CH_4, an experiment equivalent to that shown in Fig. 7 was carried out, but without prior adsorption of NO. Figure 8 shows the results. CO is observed in the gas phase above 610 K and CO_2 above 775 K. Significant CH_4 consumption occurs above 775 K. It is evident, therefore, that Pd dispersed as $Z^-H^+[Pd(OH)]^+Z^-$ can be reduced by CH_4 above 610 K. The total amount of oxygen (as O atoms) removed as CO and CO_2 is equal to 3.4 μmol. The total amount of Pd in the sample is 4.1 μmol, yielding an O/Pd

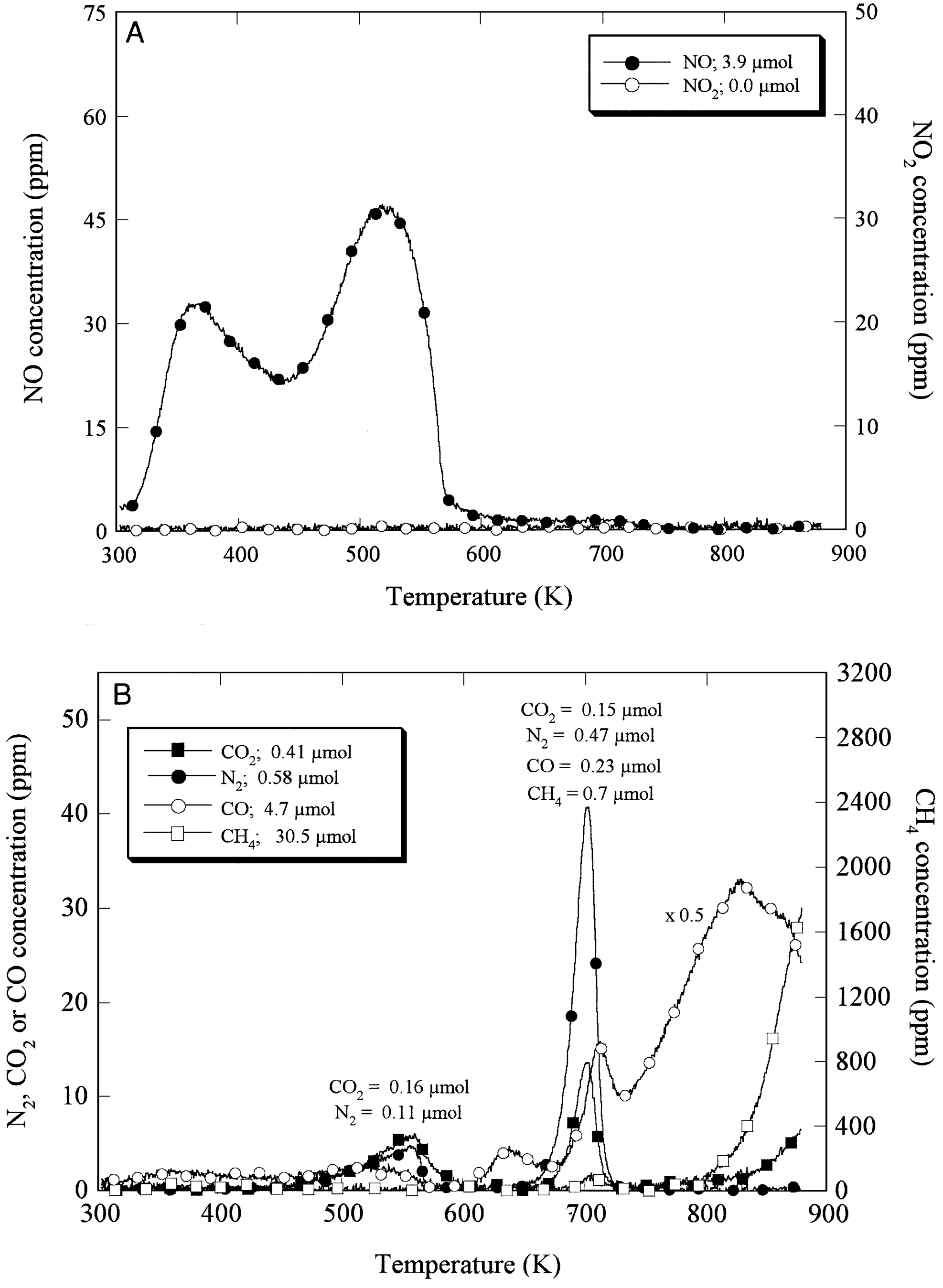

FIG. 7. (A) Mass spectrometer signals for NO and NO_2 observed during temperature-programmed desorption into 1% CH_4 in He following room temperature exposure of the catalyst to 5000 ppm NO for 20 min. The total quantities of NO and NO_2 desorbed are given in the inset. (B) Mass spectrometer signals for CO_2, N_2, CO, and CH_4 observed during temperature-programmed desorption into 1% CH_4 in He following room temperature exposure of the catalyst to 5000 ppm NO for 20 min. The total quantities of CO_2, N_2, CO, and CH_4 formed/consumed are given in the inset.

ratio of 0.83. Note also in both Figs. 7B and 8 that the total amount of CH_4 consumed is much larger than the total amount of carbon observed in the gas phase as CO or CO_2, suggesting significant dissociation of CH_4 to produce carbonaceous species. Similar results have been reported for Pd-Na-ZSM-5 (22) and it has been demonstrated that it is possible to deposit coke on a supported Pd catalyst by exposing it to CH_4 at 773 K for 30 min (23). Accordingly, the results presented in Fig. 8 can be interpreted as follows. Above 610 K the highly dispersed Pd undergoes reduction to form small Pd clusters within the pores of the zeolite (*viz.*, $CH_4 + 4\ Z^-H^+[Pd(OH)]^+Z^- \rightarrow 8\ H^+Z^- + 4\ Pd_s +$

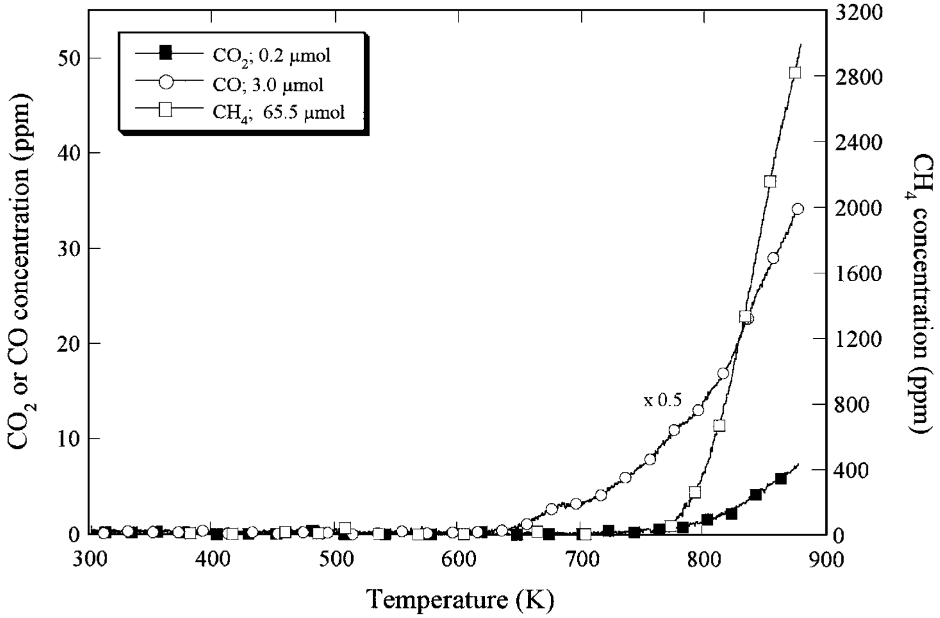

FIG. 8. Mass spectrometer signals for CO_2, CO, and CH_4 observed during a temperature ramp in 1% CH_4 in He. The total quantities of CO_2, CO, and CH_4 formed/consumed are given in the inset.

2 $H_2O + CO_2$). Carbon deposition then occurs on the surface of these particles above 775 K via the decomposition of CH_4 (*viz.*, $CH_4 \rightarrow CH_{x,s} + (2 - x/2)\ H_2$).

As with the TPD-IR experiment, the temperature-programmed desorption of NO (TPD-MS) into 1% CH_4 + 1% O_2 (not shown) is similar to the TPD-MS into 1% CH_4 (Fig. 7). However, NO_2 is observed in the gas phase between 430 K and 575 K and NO is also seen in the gas phase beginning at 700 K and continuing to temperatures greater than 873 K. N_2 is observed in the gas phase between 460 K and 575 K, and again beginning at 650 K and continuing to temperatures of more than 873 K. CO_2 production and CH_4 and O_2 consumption begin at about 600 K and in this case the primary reaction occurring is $CH_4 + 2\,O_2 \rightarrow CO_2 + 2\,H_2O$ (this is also observed in the absence of preadsorbed NO). Reduction of adsorbed NO occurs concurrently but the temperature range over which N_2 is formed is much broader than when O_2 is absent from the feed. This difference is attributed to the lower concentration of CH_4 in the gas phase due to the rapid rate of CH_4 combustion by O_2 in the temperature regime where NO reduction occurs. The total amount of nitrogen (as N) observed is 4.6 μmol.

Summary of NO TPD Experiments

Figure 9 shows the integrated area of the band at 1881 cm^{-1} ($Z^-H^+[Pd(OH)(NO)]^+Z^-$) observed during the NO TPD-IR experiments as a function of temperature for temperatures above 423 K, since this is the only type of NO species observed in this temperature range. At 423 K in all gas mixtures, the intensity of this band is the same. However, as the temperature is increased, there are notable differences. In He, the band intensity decreases monotonically above 423 K. When O_2 is added to the He carrier, the decline in intensity is similar to that in He below 673 K, but it occurs more rapidly at higher temperatures. When the carrier gas contains CH_4, the intensity of the nitrosyl signal increases slightly up to a temperature of about 673 K and then rapidly decreases as the temperature rises further. When O_2 is present, together with CH_4 in the carrier, there is again an initial rise in the intensity of the NO signal, followed by a more progressive decrease above 573 K.

NO_2 TPD in He

Figure 10 shows the infrared spectra acquired during temperature-programmed desorption into He following room-temperature adsorption of NO_2 for 20 min from a stream containing 1% NO_2 in He. At 423 K, bands are observed at 1656, 1642, 1621, and 1586 cm^{-1} attributable to NO_2 and NO_3 species (24). The features at 1656, 1621, and 1586 cm^{-1} disappear above 523 K, and the only feature remaining is that at 1642 cm^{-1} due to a strongly adsorbed NO_2 (24). At temperatures above 623 K the band at 1642 cm^{-1} disappears, and a new band due to the Pd nitrosyl appears at 1865 cm^{-1} ($Z^-H^+[Pd(OH)(NO)]^+Z^-$). As the temperature is increased, the intensity of the band at 1865 cm^{-1} goes through a maximum at 723 K and is still present at 773 K.

NO_2 TPD in CH_4

The infrared spectra acquired during the temperature-programmed desorption of NO_2 into CH_4 are shown in

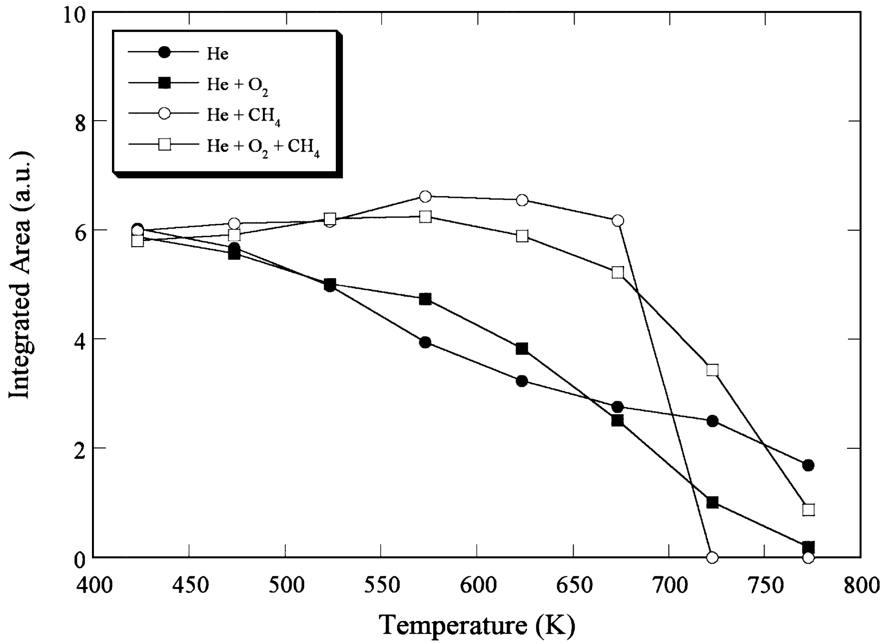

FIG. 9. Integrated area of the band observed at 1881 cm^{-1} during NO temperature-programmed desorption experiments as a function of temperature.

Fig. 11. At temperatures less than 473 K the appearance of the infrared spectra is similar to those shown in Fig. 10. At higher temperatures, however, the band at 1642 cm^{-1} decreases in intensity more rapidly than in a He purge, and the band at 1865 cm^{-1} first appears at a lower temperature, 523 K. In comparison with the desorption into He, the band at 1865 cm^{-1} grows to a greater intensity in the presence of CH$_4$, but is completely removed from the catalyst above 673 K. A blowup of spectra observed at 673 K and above is shown in Fig. 11B. Bands for NCO (2300 cm^{-1}) and CO$_2$ (doublet centered at 2347 cm^{-1}) are apparent at 673 K, and at 723 K bands for NCO, CO$_2$, and CN (2142 cm^{-1}) are observed.

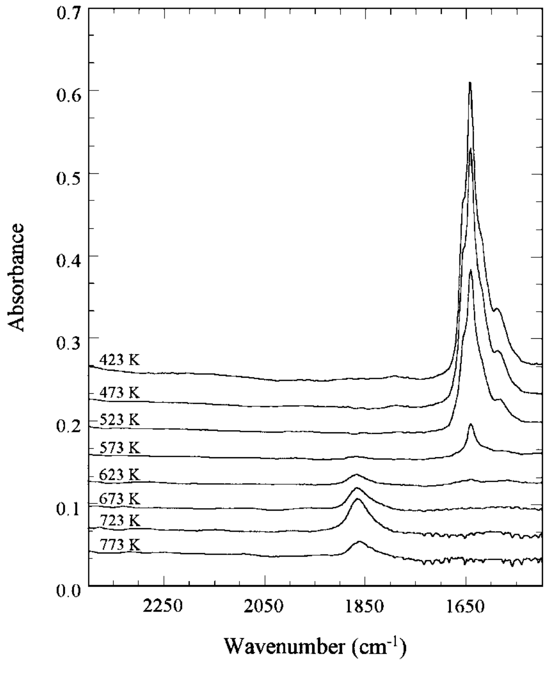

FIG. 10. Infrared spectra taken during temperature-programmed desorption into He following room-temperature exposure of the catalyst to 1% NO$_2$ for 20 min.

NO TPR in CH$_4$

Figure 12A shows the infrared spectra taken during the temperature-programmed heating of the catalyst while flowing 5000 ppm NO and 1% CH$_4$. The room temperature spectrum is slightly different from that shown in Fig. 4; an additional shoulder is present at 1818 cm^{-1}. This feature may be due to bent NO on Pd, as suggested by previous work on Pd-Y, in which a band at 1780 cm^{-1} was assigned to bent NO (25). The band at 1818 cm^{-1} disappears by 323 K. The feature at 2133 cm^{-1} goes through a maximum at 323 K and is gone above 623 K. There is, again, a single band at 1638 cm^{-1} due to H$_2$O. Below 623 K, these spectra are identical to those obtained during NO TPR (not shown). At temperatures greater than 623 K, the nitrosyl band appears more intense than when the experiment is carried out in flowing NO alone. At 773 K, the nitrosyl intensity is about 1.3 times that observed in an NO TPR experiment. Figure 12B shows a blowup of the spectra taken above 523 K. Above 573 K, the band at 2300 cm^{-1} is again present; however, the band at 2142 cm^{-1} is not observed. The absence of a band at 2142 cm^{-1} due to CN may be because this species reacts rapidly with NO.

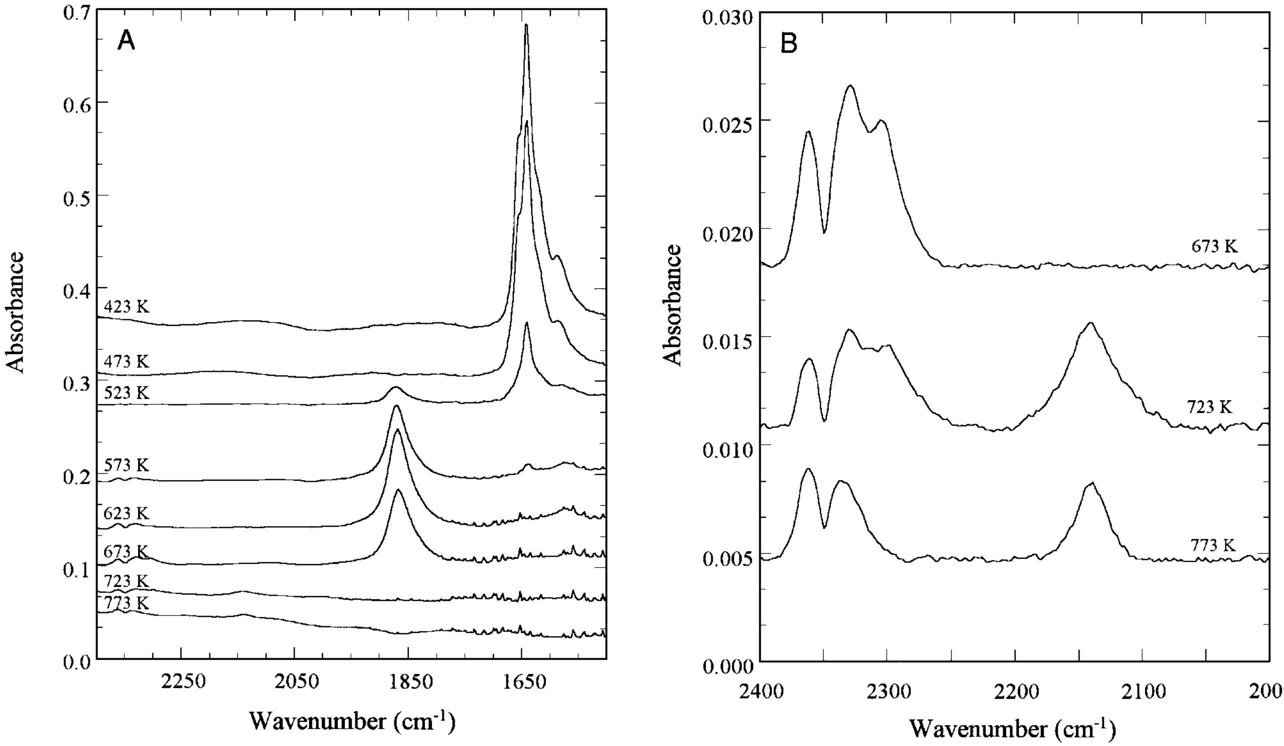

FIG. 11. (A) Infrared spectra taken during temperature-programmed desorption into 1% CH_4 in He following room-temperature exposure of the catalyst to 1% NO_2 for 20 min. (B) Blowup of spectra taken at 673 K and above during temperature-programmed desorption into 1% CH_4 in He following room-temperature exposure of the catalyst to 1% NO_2 for 20 min.

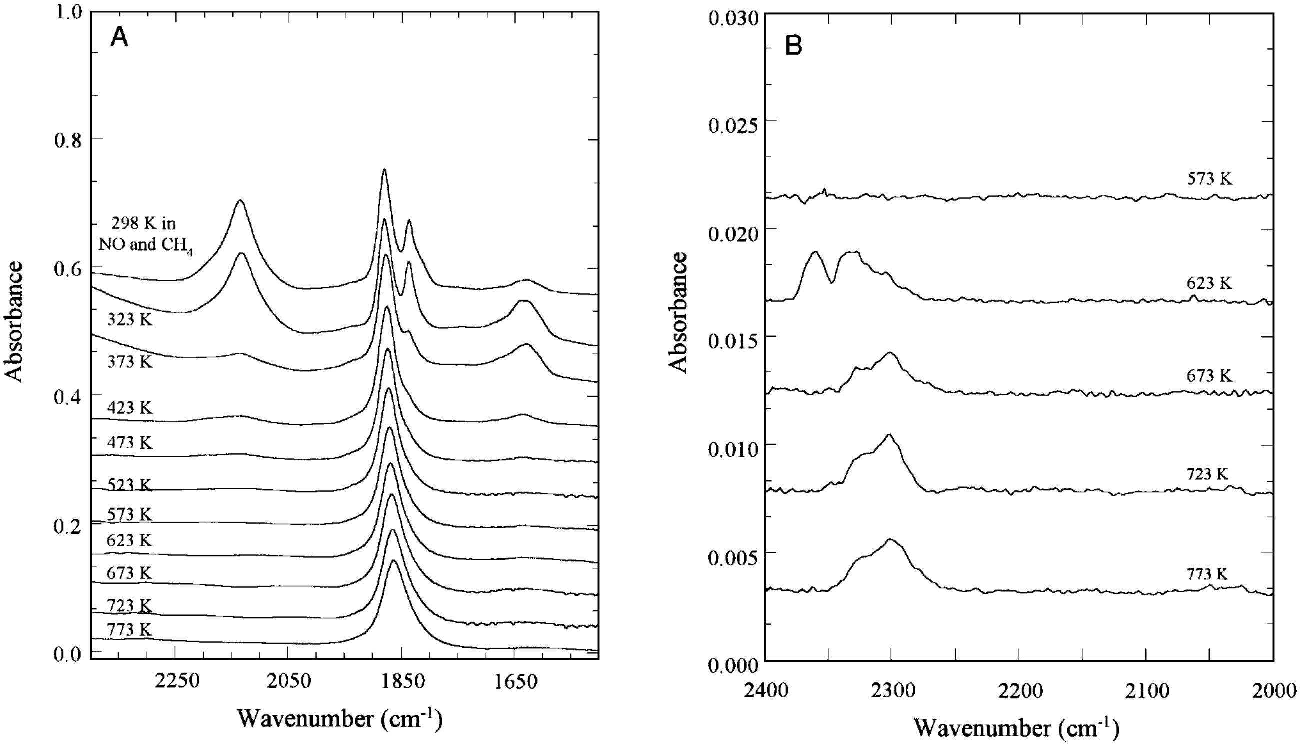

FIG. 12. (A) Infrared spectra taken during a temperature ramp while 5000 ppm NO and 1% CH_4 is passed over the catalyst after it had been exposed to this mixture at room temperature for 20 min. (B) Blowup of the infrared spectra taken at 573 K and above while 5000 ppm NO and 1% CH_4 is passed over the catalyst after it had been exposed to this mixture at room temperature for 20 min.

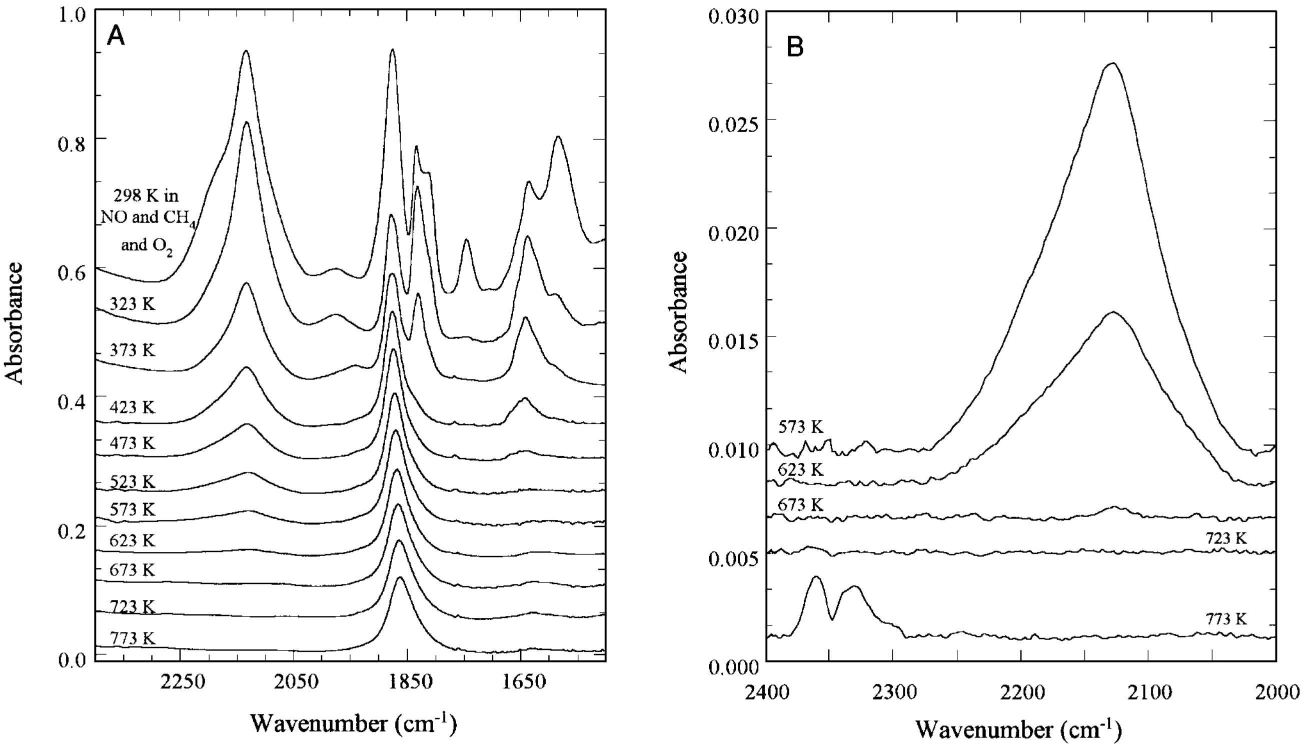

FIG. 13. (A) Infrared spectra taken during a temperature ramp while 5000 ppm NO, 1% O_2, and 1% CH_4 is passed over the catalyst after it had been exposed to this mixture at room temperature for 20 min. (B) Blowup of the infrared spectra taken at 573 K and above while 5000 ppm NO, 1% O_2, and 1% CH_4 is passed over the catalyst after it had been exposed to this mixture at room temperature for 20 min.

NO TPR in CH_4 and O_2

Figure 13A shows the data acquired during the temperature-programmed heating of the catalyst while flowing a mixture containing 5000 ppm NO, 1% O_2, and 1% CH_4. At room temperature, nitrosyl bands are observed at 1875, 1833, and 1811 cm^{-1} (the same as previously described just slightly shifted) along with the band at 2133 cm^{-1} due to NO^+. New bands are observed at 2190, 1746, 1636, and 1584 cm^{-1}. The band at 2190 cm^{-1} is due to NO_2 adsorbed on protons in the zeolite (26, 27) and the band at 1636 cm^{-1} is due to strongly adsorbed NO_2 on Pd. The sharp band at 1746 cm^{-1} can be assigned to N_2O_4 (28) and the band at 1584 is assigned to N_2O_3 (29, 30). The features at 2190 and 1746 cm^{-1} are gone at 323 K, and species contributing to the bands at 1833, 1811, and 1584 cm^{-1} are no longer evident at 423 K. The band at 1636 cm^{-1} disappears at 523 K. Below 573 K the spectra are identical to those observed during the NO TPR in 1% O_2 (not shown). Figure 13B shows a blowup of the spectra observed at temperatures of 573 K and higher. The band at 2133 cm^{-1} due to NO^+ is not evident at 673 K. This observation differs from that made during NO TPR in 1% O_2, where it was observed that the band at 2133 cm^{-1} persisted up to 773 K. The band at 1881 cm^{-1} due to nitrosyl species is still present at 773 K and is smaller in CH_4 and O_2 than in CH_4 alone (but is still greater than when CH_4 is completely absent). The bands at 2300 and 2142 cm^{-1} are not present at any temperature.

Summary of NO TPR Experiments

Figures 14A and B present the integrated areas of the bands at 1881 cm^{-1} and 2133 cm^{-1}, respectively, as functions of temperature for all of the TPR-IR experiments. It is seen in Fig. 14A that the intensity of the band at 1881 cm^{-1} decreases more rapidly with increasing temperature when NO and O_2 are both present in the gas phase. This effect is probably due to the partial conversion of NO to NO_2, which causes a reduction in the partial pressure of NO. When CH_4 is present with NO, either in the absence or presence of O_2, the intensity of the band at 1881 cm^{-1} is always higher than that observed when CH_4 is absent. This may be due to the higher gas phase concentration of NO caused by the reduction of NO_2 to NO.

As seen in Fig. 14B, the band at 2133 cm^{-1} due to NO^+ is seven times larger than that observed in the absence of O_2. This is not surprising, since, as discussed above, a recent study has shown that O_2 accelerates the replacement of protons by NO^+ via the reaction $2\ NO + 1/2\ O_2 + 2\ Z^-H^+ \rightleftharpoons H_2O + 2\ Z^-NO^+$. When O_2 is absent, the presence of CH_4 in the gas phase has no effect on the intensity of the NO^+ band, irrespective of the temperature. When O_2

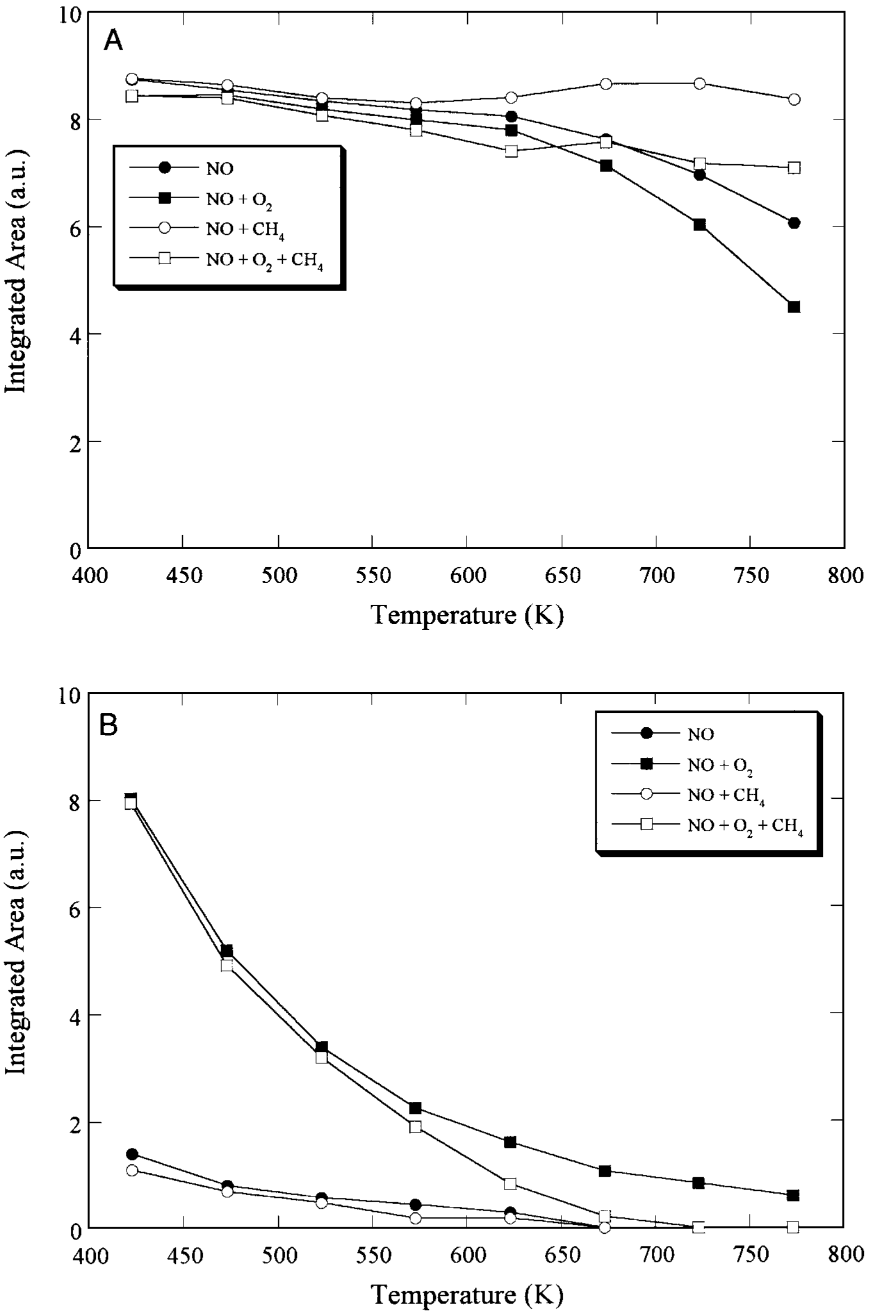

FIG. 14. (A) Integrated area of the band observed at 1881 cm^{-1} during NO temperature-programmed desorption experiments as a function of temperature. (B) Integrated area of the band observed at 2133 cm^{-1} during NO temperature-programmed desorption experiments as a function of temperature.

is present, together with CH_4 and NO, the intensity of the NO^+ band is the same as in the absence of CH_4 at 423 K; however, the intensity of this band decreases more rapidly with increasing temperature. This trend might be attributed to (1) the lower concentration of NO at higher temperatures, resulting from the reduction of NO, and (2) the higher concentration of H_2O due to the combustion of CH_4 which results in the displacement of NO^+ from the surface via the reaction shown previously.

DISCUSSION

The reduction of NO can occur over both H-ZSM-5 and Pd-H-ZSM-5. Reference to Figs. 1 and 2 shows that above 600 K Pd-H-ZSM-5 is up to three times as active as H-ZSM-5 when comparison is made on a per gram basis. Since the ratio of Pd to Al atoms in Pd-H-ZSM-5 is 0.048 and the ratio of Brønsted acid protons to Al is assumed to be 1.0 in H-ZSM-5, the ratio of turnover frequencies is estimated to range from 88 at 673 K to 36 at 873 K. Thus, it is clear that on a per site basis the activity of Pd^{2+} cations is considerably higher than that of Brønsted acid protons.

The state of Pd in Pd-H-ZSM-5 is a strong function of conditions. Figure 3 shows that under reaction conditions when O_2 is present, the portion of the Pd present as $Z^-H^+[Pd(OH)]^+Z^-$ remains in this state and does not undergo reduction, independent of the reaction temperature. However, in the absence of O_2, $Z^-H^+[Pd(OH)]^+Z^-$ is reduced and can form small particles of Pd at temperatures between 610 K and 873 K. The reducibility of $Z^-H^+[Pd(OH)]^+Z^-$ by CH_4 is confirmed by the experiments shown in Figs. 7B and 8, which demonstrate that reduction occurs at temperatures above 610 K. A proposed set of elementary steps describing this process is shown in Fig. 15. Methane attacks $Z^-H^+[Pd(OH)]^+Z^-$ and reduces Pd(OH) to Pd(H) (reaction 1) followed by the loss of the H_2 yielding CH species on the surface (reaction 2). This species then reacts with H_2O to form adsorbed CO with the release of another H_2 (reaction 3). CO then desorbs (reaction 4) and can react with $Z^-H^+[Pd(OH)]^+Z^-$ to yield CO_2 and $Z^-H^+[Pd(H)]^+Z^-$ (reaction 5). H_2 can also react with $Z^-H^+[Pd(OH)]^+Z^-$ to form another $Z^-H^+[Pd(H)]^+Z^-$ and H_2O (reaction 6). Pd atoms formed by autoreduction of $Z^-H^+[Pd(H)]^+Z^-$ can agglomerate to form small particles of Pd occluded within the channels and channel intersections of the zeolite (reaction 7). As discussed previously (7), Pd particles occluded in this manner do not readily adsorb CO, and hence, the ratio of adsorbed CO to Pd is expected to decrease, as is observed in Fig. 3. In light of these observations, the mechanism of NO reduction by CH_4 can be expected to change, depending on the presence or absence of O_2 in the feed (see below).

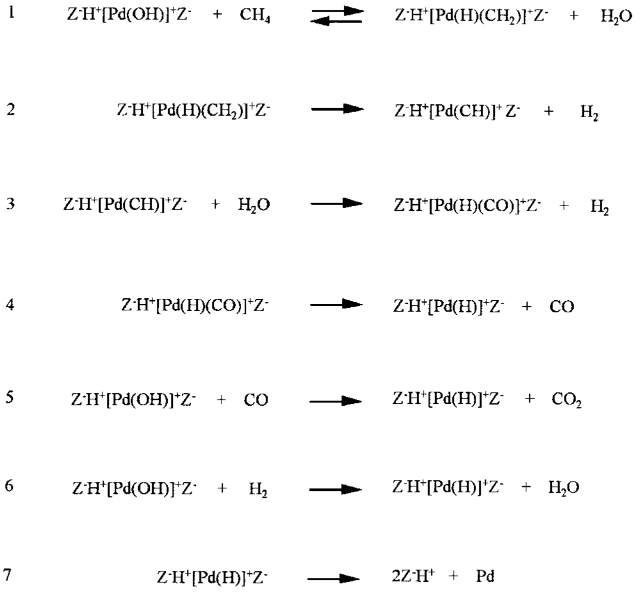

FIG. 15. Proposed elementary steps for the reduction of $Z^-H^+[Pd(OH)]^+Z^-$ by CH_4.

Infrared spectroscopy reveals the presence of three principal forms of nitrogen-containing species: (1) nitrito species present as $Z^-H^+[Pd(OH)(ONO)]^+Z^-$; (2) NO^+ cations present as Z^-NO^+; and (3) nitrosyl species present as $Z^-H^+[Pd(OH)(NO)]^+Z^-$. The relative stability and reactivity of these species is examined next, with the objective of identifying which of these species is involved in the steady-state reduction of NO by CH_4.

Evidence for nitrito species is seen primarily upon the adsorption of NO_2 (see Figs. 10 and 11) or upon adsorption of NO in the presence of O_2 (see Figs. 12 and 13). The infrared bands below 1650 cm^{-1} associated with these species disappear above 523 K with the concurrent appearance of a band at 1865 cm^{-1} for adsorbed NO. The desorption of NO_2 between 475 K and 625 K is observed during the TPD of adsorbed NO (see Fig. 5), but in this case NO_2 may be formed via disproportionation of NO, since infrared spectra taken during NO desorption show little, if any evidence for adsorbed NO_2 over this temperature range (see Fig. 4). CH_4 reacts with adsorbed NO_2 as evidenced by the conversion of nitrito species to nitrosyl species at temperatures above 473 K (see Fig. 11) and an increase in the disappearance of the infrared band for nitrito species. The temperature-programmed reaction of adsorbed NO also shows that NO_2 will react with CH_4 in the temperature range of 500 K to 600 K (see Fig. 7B). Based on this evidence, it is concluded that nitrito species are not present under the conditions of steady-state NO reduction by CH_4, which occurs above 650 K.

NO^+ species are formed at room temperature much more rapidly in the presence than in the absence of O_2. As noted earlier, these species are believed to be formed via the reaction $2\,NO + 1/2\,O_2 + 2\,Z^-H^+ \rightleftharpoons H_2O + 2\,Z^-NO^+$ (20). The water released in this reaction can hydrogen bond to Brønsted acid sites, giving rise to the band at 1638 cm^{-1}. The progressive disappearance of NO^+, which is characterized by the infrared band at 2133 cm^{-1}, upon heating of adsorbed NO in He is attributed to a reversal of the process by which NO^+ was first formed. As shown in Fig. 14B, NO^+ does not react with CH_4. The lowering in the band intensity for NO^+ when an $NO/O_2/CH_4$ mixture is heated as compared to an NO/O_2 mixture is attributed to the high concentration of H_2O in the former mixture, in as much as H_2O contributes to the destruction of NO^+, as noted above. Based on these considerations, NO^+ is not believed to be a critical species in the reduction of NO by CH_4 under steady-state conditions.

Molecularly adsorbed NO is present in three forms as evidenced by the presence of infrared bands at 1818 cm^{-1}, 1836 cm^{-1}, and 1881 cm^{-1}. The species associated with the first two features are very weakly bound and are absent above 423 K. The band at 1881 cm^{-1} is attributable to a form of adsorbed NO which remains strongly bound up to

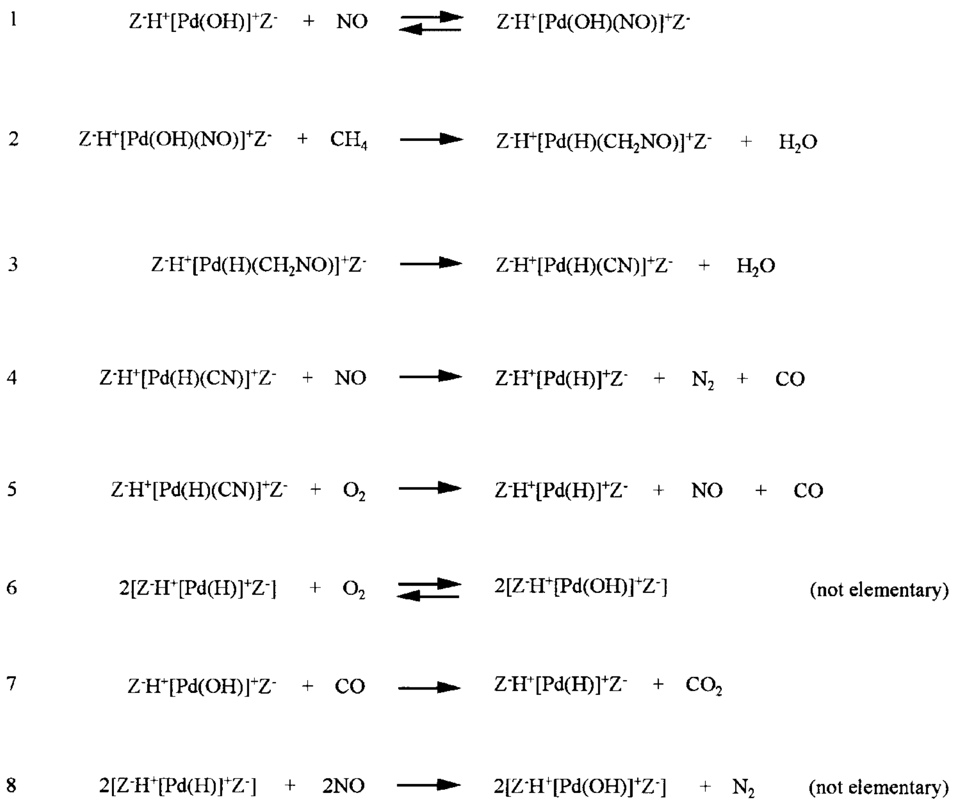

FIG. 16. Proposed mechanism for NO reduction by CH_4 over Pd-H-ZSM-5 in the presence of O_2.

temperatures of 773 K. TPD studies show that this form of adsorbed NO will react with CH_4 above 650 K, either in the absence or presence of O_2. These observations indicate that the reduction of NO by CH_4 is initiated by the interaction of CH_4 with adsorbed NO rather than NO_2, as has been suggested previously for Pd-H-ZSM-5 (2, 9, 10) and observed by *in situ* infrared spectroscopy in studies conducted with Co-ZSM-5 and Mn-ZSM-5 (12, 13).

Figure 16 illustrates a possible mechanism for the reduction of NO by CH_4 in the presence and absence of O_2. The sequence begins with the adsorption of NO as $Z^-H^+[Pd(OH)(NO)]^+Z^-$ (reaction 1). Adsorbed nitrosyl species then react with CH_4 to produce CH_2NO (or its isomer CHNOH) with the release of water (reaction 2). Note that the formation of CH_2NO results in the replacement of OH^- by H^- in the coordination sphere of Pd^{2+}. CH_2NO present as a ligand in Co complexes is known to decompose releasing water and leaving behind a CN (neutral) group as a ligand (31). Accordingly, it is proposed that a similar reaction occurs over Pd-H-ZSM-5 (reaction 3). The CN species can then react with either NO or O_2 (if present). Reaction with NO (reaction 4) is envisioned to form N_2 and CO, whereas reaction with O_2 (reaction 5) is assumed to produce NO and CO. Both reactions have been observed to occur during NO reduction by CH_4 over Co-ZSM-5 and Mn-ZSM-5 (12, 13), as well as in the present study. While the reaction of CN species with NO_2 to form N_2 and CO_2 was not investigated for Pd-H-ZSM-5, this reaction was found to be significantly faster than the reaction of CN species with NO or O_2 for Co-ZSM-5 and Mn-ZSM-5 (12, 13). Therefore, since NO_2 will be present in the gas phase when NO and O_2 are present together, it is quite conceivable that the reaction of NO_2 with CN species occurs and will also be very rapid for Pd-H-ZSM-5. The CO produced by reactions 4 and 5 can react with $Z^-H^+[Pd(OH)]^+Z^-$ to form CO_2 and $Z^-H^+[Pd(H)]^+Z^-$ (reaction 7). The latter species are assumed to undergo reaction with O_2 or NO to reform $Z^-H^+[Pd(OH)]^+Z^-$ (reactions 6 and 8). $Z^-H^+[Pd(H)]^+Z^-$ can also undergo autoreduction with the resulting release of Pd atoms which can then agglomerate into small Pd particles (see Fig. 15). The data presented in Fig. 3 indicate that in the absence of O_2 in the feed, Pd^{2+} cations undergo reduction during the reaction of NO with CH_4 at temperatures above about 610 K. Since the reduction of Pd^{2+} does not occur when O_2 is present, this suggests that O_2 is more effective than NO in restoring $Z^-H^+[Pd(H)]^+Z^-$ to $Z^-H^+[Pd(OH)]^+Z^-$.

If particles of metallic Pd are formed, NO reduction can still occur. In this case, it has been proposed (22) that NO reduction is initiated by the dissociative adsorption of NO. N_2 results from the recombination of adsorbed N atoms, and CO_2 and H_2O are formed by the reaction of CH_4 with adsorbed O atoms. In the presence of O_2, Pd particles are rapidly oxidized to PdO, which is a very effective catalyst for the combustion of CH_4 by O_2. As a consequence, the formation of PdO leads to a decrease in the concentration of CH_4 and, hence, to a reduction in the rate of NO reduction on any Pd^{2+} cations remaining in the catalyst (6).

Finally, we note that the scheme presented in Fig. 16 indicates that reduction of adsorbed NO by CH_4 should result in the formation of CO and CO_2 in the stoichiometric reactions:

$$2\,Z^-H^+[Pd(OH)(NO)]^+Z^- + Z^-H^+[Pd(OH)]^+Z^- + CH_4 \rightarrow 3\,Z^-H^+[Pd(H)]^+Z^- + N_2 + CO + 2\,H_2O \quad [1]$$

$$2\,Z^-H^+[Pd(OH)(NO)]^+Z^- + 2\,Z^-H^+[Pd(OH)]^+Z^- + CH_4 \rightarrow 4\,Z^-H^+[Pd(H)]^+Z^- + N_2 + CO_2 + 2\,H_2O \quad [2]$$

Since the ratio of N_2/CO and N_2/CO_2 is unity for both reactions, it is expected that the experimentally observed value of N_2/CO_x should also be one. The results presented in Fig. 7B show that the N_2/CO_x ratio is equal to 1.2 for reduction occurring in the temperature interval of 650–720 K, in rough agreement with reactions 1 and 2 above.

CONCLUSIONS

The state of Pd in Pd-H-ZSM-5 during the reduction of NO by CH_4 is strongly dependent on the reaction temperature and the presence or absence of O_2 in the gas phase. Below approximately 610 K, Pd remains highly dispersed as $Z^-H^+[Pd(OH)]^+Z^-$ species, but at temperatures above 610 K these species undergo reduction to form small particles of Pd when O_2 is absent from the gas phase. When NO reduction occurs in the presence of O_2, most of the Pd remains dispersed as $Z^-H^+[Pd(OH)]^+Z^-$ up to 873 K.

Comparison of the activities of H-ZSM-5 and Pd-H-ZSM-5 for NO reduction by CH_4 in the presence of O_2 reveals that the activity of dispersed Pd^{2+} cations is 36 to 88 times higher than that of Brønsted acid protons. Thus, the principal active component in Pd-H-ZSM-5 is Pd^{2+}.

In situ infrared spectra taken at temperatures above 673 K, where significant NO reduction occurs, reveal evidence for NO^+ and NO as the principal adsorbed species. Adsorbed NO^+ does not react with CH_4 at temperatures up to 773 K, whereas adsorbed NO reacts at temperatures above 650 K. CN species are formed during the reduction of NO and are found to be highly reactive with both NO and O_2. The mechanism presented in Fig. 16 has been proposed to explain the reduction of NO by CH_4 both in the absence and presence of O_2.

ACKNOWLEDGMENTS

This work was supported by the Director of the Office of Basic Energy Sciences, Chemical Sciences Division, of the U.S. Department of Energy under Contract DE-AC03-76SF00098.

REFERENCES

1. Nishizaka, Y., and Misono, M., *Chem. Lett.*, 1295 (1993).
2. Nishizaka, Y., and Misono, M., *Chem. Lett.*, 2237 (1994).
3. Loughran, C. J., and Resasco, D. E., *Appl. Catal. B: Env.* **7**, 113 (1995).
4. Adelman, B. J., and Sachtler, W. M. H., *Appl. Catal. B: Env.* **14**, 1 (1997).
5. Descorme, C., Fakche, A., Garbowski, E., Lecuyer, C., and Primet, M., *in* "Proceedings of the International Gas Research Conference, France, 1995," p. 505.
6. Ali, A., Alvarez, A., Loughran, C. J., and Resasco, D. E., *Appl. Catal. B: Env.* **14**, 13 (1997).
7. Aylor, A. W., Lobree, L. J., Reimer, J. A., and Bell, A. T., *J. Catal.* **172**, 453 (1997).
8. Rice, M. J., Chakraborty, A. K., and Bell, A. T., unpublished.
9. Misono, M., Hirao, Y., and Yokoyama, C., *Catal. Today* **38**, 157 (1997).
10. Kato, H., Yokoyama, C., and Misono, M., *Catal. Lett.* **47**, 189 (1997).
11. Joly, J. F., Zanier-Szyldowski, N., Colin, S., Raatz, F., Saussey, J., and Lavalley, J. C., *Catal. Today* **9**, 31 (1991).
12. Aylor, A. W., Lobree, L. J., Reimer, J. A., and Bell, A. T., *in* "11th International Congress on Catalysis-40th Anniversary" (J. W. Hightower, W. N. Delgass, E. Iglesia, and A. T. Bell, Eds.), Studies in Surface Science and Catalysis, Vol. 101, p. 661. Elsevier, Amsterdam, 1996.
13. Aylor, A. W., Lobree, L. J., Reimer, J. A., and Bell, A. T., *J. Catal.* **170**, 390 (1997).
14. Descorme, C., Gelin, P., Primet, M., and Lecuyer, C., *Catal. Lett.* **41**, 133 (1996).
15. Parker, L. M., Bibby, D. M., and Burns, G. R., *Zeol.* **13**, 107 (1993).
16. Iwamoto, M., Yahiro, H., Mizuno, N., Zhang, W.-X., Mine, Y., Furukawa, H., and Kagawa, S., *J. Phys. Chem.* **96**, 9360 (1992).
17. Giamello, E., Murphy, D., Magnacca, G., Morterra, C., Shioya, Y., Nomura, T., and Anpo, M., *J. Catal.* **136**, 510 (1992).
18. Valyon, J., and Hall, W. K., *J. Phys. Chem.* **97**, 1204 (1993).
19. Hoost, T. E., Laframboise, K. A., and Otto, K., *Catal. Lett.* **33**, 105 (1995).
20. Hadjiivanov, K., Saussey, J., Freysz, J. L., and Lavalley, J. C., *Catal. Lett.* **52**, 103 (1998).
21. Lobree, L. J., Aylor, A. W., Reimer, J. A., and Bell, A. T., *J. Catal.* **169**, 188 (1997).
22. Loughran, C. J., and Resasco, D. E., *Appl. Catal. B: Environ.* **5**, 351 (1995).
23. Solymosi, F., Erdöhelyi, A., Cserényi, J., and Felvégi, A., *J. Catal.* **147**, 272 (1994).
24. Nakamoto, K., "Infrared and Raman Spectra of Inorganic and Coordination Compounds," 4th ed. Wiley, New York, 1986.
25. Che, M., Dutel, J. F., Gallezot, P., and Primet, M., *J. Phys. Chem.* **80**, 2371 (1976).
26. Evans, J. C., Rinn, H. W., Kuhn, S. J., and Olah, G. A., *Inorg. Chem.* **3**, 857 (1964).
27. Nebgen, J. W., McElroy, A. D., and Klodowsky, H. F., *Inorg. Chem.* **4**, 1796 (1965).
28. Begun, G. M., and Fletcher, W. H., *J. Molec. Spec.* **4**, 388 (1960).
29. Chao, C.-C., and Lunsford, J. H., *J. Am. Chem. Soc.* **93**, 71 (1971).
30. Hisatsune, I. C., and Devlin, J. P., *Spectrochimica Acta* **16**, 401 (1960).
31. Chang, J., Seidler, M. D., and Bergman, R. G., *J. Am. Chem. Soc.* **111**, 3258 (1989).